ARPN Journal of Engineering and Applied Sciences

www.arpnjournals.com

FINITE ELEMENT MODELING OF STRESS DISTRIBUTION IN THE CUTTING PATH IN MACHINING OF DISCONTINUOUSLY REINFORCED ALUMINIUM COMPOSITES

Raviraj Shetty[1], Laxmikant K.[1], R. Pai[1] and S. S. Rao[2]
[1]Department of Mechanical and Manufacturing Engineering, Manipal Institute of Technology, Karnataka, India
[2]Department of Mechanical Engineering, National Institute of Technology, Karnataka, India
E-Mail: rrshetty2@rediffmail.com

ABSTRACT

One focus of this paper is to highlight issues on machining of discontinuously reinforced aluminium composites (DRACs), due to the complex deformation and interactions among particles, tool and matrix it is often unable to explore the behavior by an experimental or analytical method. This paper investigates the stress distribution in particles along, above and below cutting path under different cutting speed and constant depth of cut using finite element method. The development of stress fields in the DRACs was analyzed and physical phenomena such particle de-bonding, displacements and inhomogeneous deformation of matrix material were explored. It was found that tool-particle interaction and stress distributions in the particles/matrix are responsible for particle de-bonding and surface damage during machining of DRACs.

Keywords: modeling, aluminium, composites, finite element, machining, stress distribution, tool, particle, interaction.

Nomenclature

σ_y = Yield stress.
σ_o = Initial yield stress
ε = Strain rate
C and P = Cowper-Symonds parameters for strain rate.
e_{eff} = Effective plastic strain.
β = Hardening parameter.
E_P = Plastic hardening modulus.
E_{tan} = Tangent modulus.
E = Modulus of elasticity
τ_{lim} = Limiting shear stress
τ = Equivalent shear stress
P = Contact pressure
μ = Friction of coefficient
b = Cohesion sliding resistance

1. INTRODUCTION

A Discontinuously Reinforced Aluminium Composites can be described as a material which is made up of a continuous metallic phase (the matrix) into which a second phase (or phases) has been artificially introduced. Early DRACs had their application confined to military and aerospace applications, their extensive usage was hindered due to their high production costs, limited production methods, and restricted product forms [Evans *et al.* (2003)].

In a monolithic metal, matrix metal is the load transferor as well as a load carrier. However, the nature of load bearing by a composite depends on the type of its components. For a discontinuous particle-reinforced MMC, both the matrix and reinforcement are the load carriers and load transferors [Huda *et al.* (1994)].

Prior to 1983, there was no literature related to the finite-element simulation of stress distributions in metal cutting incorporating plasticity theory. Few milestones in this particular area have been cited. A pioneering piece of work was carried out by [Iwata *et al.* (1984)] to model the orthogonal cutting, assuming plane-strain conditions, to predict chip shape, and stress and strain distributions. Chip fracture was also analyzed by combining with different ductile failure criteria.

The machining mechanism of Discontinuously Reinforced Aluminium Composites is expected to be different from others. Numerous reports can be found in the literature describing the experimental studies related to the machining of MMCs, but analytical and numerical investigations are few. [Monaghan and Brazil (1997)] modeled the machining (by FORGE2 code) of A356 aluminum alloy and then submodeled (by ANSYS software) different regions of the chip and the machined surface of MMC. [Ramesh *et al.*, (2001)] carried out a transient dynamic finite-element analysis to investigate the mechanics of diamond turning of an Al6061/SiC MMC. They studied the possible encounters of the tool that included tool facing SiC/matrix and tool ploughing SiC/matrix, and considered frictionless point contact between the tool and workpiece. They presented the range of forces and stresses that could be generated during micro-machining of MMC. [Zhu and Kishawy (2005)] developed a plane-strain thermo-elastic-plastic finite element model to simulate orthogonal machining of Al6061/Al2O3 composite using a tungsten carbide tool. They reported the average values of effective and shear stresses in the matrix and on particles at different locations in the chip and primary/secondary deformation zones, and temperature distribution in the matrix macroscopically. [Shetty *et al.* (2006)] developed a quasi static finite element code of chip separation criterion in orthogonal cutting of discontinuously reinforced aluminium composites. [Lin *et al.*, (1991)] have reported the thermal load effect and residual stresses by using thermo-elasto-

VOL. 3, NO. 4, AUGUST 2008 ISSN 1819-6608
ARPN Journal of Engineering and Applied Sciences

www.arpnjournals.com

plastic analysis. They have concluded that the effects of thermal load could be ignored for certain cutting parameter ranges. [Lin and Lin (1992)] later proposed another chip-separation criterion based on a critical value of the strain-energy density. A thermo-elasto-plastic model based on the new criterion was used to predict the stresses, strains and temperatures in the vicinity of the cutting region. They have observed that the critical value for chip separation based on energy density is a material constant and is independent of uncut chip thickness.

The main problem when machining DRACs is the extensive tool wear caused by very hard and abrasive reinforcement. Several studies have been performed in order to examine the efficiency of different cutting materials, such as cemented carbide and diamond, in turning, milling, drilling, reaming and threading of DRACs materials [Beard (1989) and Berrie (1980)]. The test result showed the influence of the reinforcement material on tool wear and the surface integrity of DRACs. In the subsurface zone, when the workpiece machined with worm cutting tools, the reinforcement are fractured. Damage of the reinforcement, caused by the machining process, can lead to significant deterioration in the properties of the component [Caprino *et al.*, (1995)].

The purpose of this paper is to investigate tool particle interaction and stress distribution during machining of DRACs with the aid of APDL code developed by ANSYS. The development of stress is explored for various cutting speed and analyzed for possible particle fracture to provide an insight for understanding the mechanism of machining DRACs.

2. FINITE ELEMENTAL MODELING

2.1 Material modeling

The DRACs work material was a 6061 aluminum alloy reinforced with 25micron silicon carbide particles size. A temperature-independent plastic kinematics material model (from ANSYS/LS-DYNA) and associative flow rule were used for the matrix. Strain rate was accounted for using the Cowper-Symonds model which scaled the yield stress by a strain rate dependent factor. According to ANSYS/LSDYNA manual the equation to calculate yield stress in the plastic kinematics material model is given below

$$\sigma y = \left[1 + \left(\frac{\dot{\varepsilon}}{C}\right)^{1/p}\right]\left(\sigma_0 + \beta E_P \varepsilon_p^{eff}\right)$$

Where

$$E_P = \left(\frac{E_{\tan} E}{E - E_{\tan}}\right)$$

Here σ_y is the yield stress, σ_0 the initial yield stress, $\dot{\varepsilon}$ the strain rate, C and P are the Cowper-Symonds strain rate parameters, εeff the effective plastic strain, β the hardening parameter (0 for kinematic hardening and 1 for isotropic hardening from ANSYS/LSDYNA manual and Ep the plastic hardening modulus, Etan the tangent modulus, E the modulus of elasticity. The material properties of the matrix were based on the commonly accepted values σ0 = 125 MPa, E = 71 GPa, Etan = 1.48 GPa from [Meijer *et al.* (2000) and Long *et al.* (2005)]. Values of Cowper-Symonds strain rate parameters (C = 6500, P = 4) for aluminum alloy were taken form ANSYS/LSDYNA manual. In this study kinematic hardening was considered as a first assumption because of comparatively low plastic hardening modulus (1.51 GPa) of matrix material and to investigate the strain rate effect.

A Strain based chip separation criterion available with ANSYS/LSDYNA for this material model was used in the simulation. According to this criterion, chip separation occurs when the strain value of the leading node is greater than or equal to a limiting value. Based on the work for aluminum alloys reported in [Zhang *et al.* (1995)], the limiting strain was taken as 1. When an element of matrix material reached the limiting strain value, the corresponding element would be deleted. Additionally, SiC particles were treated as an isotropic perfectly elastic material following the generalized Hook's law. For simplicity, particle fracture was not considered in the present model and debonding of particles was assumed to be due to failure of the matrix material around the particles. The material properties of the particles were based on the commonly accepted values: modulus of elasticity = 400 GPa and Poisson's ratio = 0.17.

2.2 Boundary conditions

A two-dimensional finite element model was constructed using explicit finite element software package ANSYS/LSDYNA, version 11. Lagrangian formulation was used for material continuum to develop the plane-stress model. The geometry of machining is shown in Figure-1. In accordance with practice, the tool cutting edge was assumed to have a 0.02 mm nose radius. The reinforcement particles were introduced around the cutting line and restricted to a small area to keep the model size manageable. In order to facilitate the study of particle interaction at different locations of the tool rake face, rows of reinforcements were perpendicular to the cutting direction. The particles (25µm diameter) were 15% by volume in this region and were assumed to be perfectly bonded with the matrix. Similar to the work reported in [Monaghan and Brazil (1997)], the interface nodes of the matrix and reinforcements were tied together, therefore the initial displacements at the interface are equal for both the matrix and reinforcements. Since the interface is very hard and brittle and hence similar to the particles [Zhu *et al.* (2005)], the interface was considered as an extension of the particle. The cutting tool was treated as a rigid body and moved horizontally into the workpiece at three different speeds i.e. 45m/min, 73m/min and 101m/min with depth of cut 0.5mm and 00 rake angle. The workpiece was fully fixed on its bottom surface to eliminate rigid body motion.

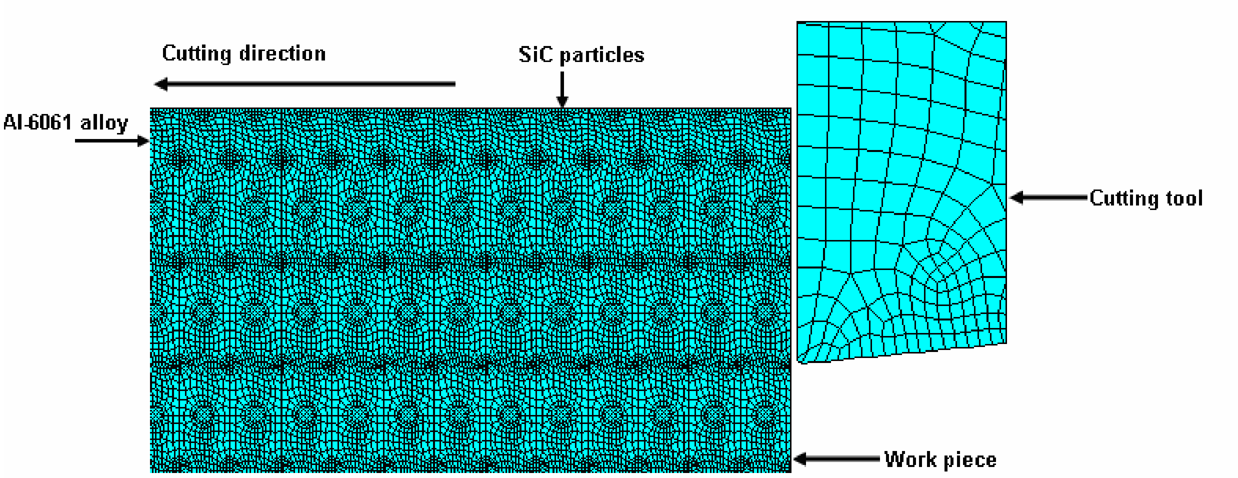

Figure-1. Finite element mesh for DRACs.

2.3 Contact and friction

Along with the general contact family in ANSYS/LSDYNA, the automatic contact options are the most commonly used contact algorithms for its versatility. Hence, 2D automatic contact was chosen for this simulation. In order to consider the effect of friction along the tool–chip interface, Coulomb friction model was employed. This is defined as

$$\tau_{\lim} = \mu P + b$$

$$|\tau| \le \tau_{\lim}$$

Where τ_{lim} is the limiting shear stress, τ the equivalent shear stress, P the contact pressure, μ the friction coefficient and b the cohesion sliding resistance (sliding resistance with zero normal pressure). According to ANSYS/LS-DYNA manual, two contacting surfaces can carry shear stresses up to a certain magnitude across their interface before they start sliding relative to each other (sticking state). When $\tau > \tau_{lim}$, the two surfaces will slide relative to each other (sliding state). For machining conditions b was assumed to be zero. The limiting shear stress τ_{lim}= 202 MPa and coefficient of friction, μ = 0.62 were based on the study reported in [Pramanik *et al.* (2006)].

3. RESULT AND DISCUSSIONS

When a cutting tool removes a layer from the DRACs, the uncut layer is first elastically deformed followed by plastic deformation and chip formation near the cutting edge of the tool. An element of material to be removed is initially under no stress when it is well ahead of the tool. As the tool approaches, the material enters a region of high strain rate where plastic deformation occurs, and becomes part of the chip. During the process of chip formation, some reinforcements in the cutting region will go into the chip, some will be debonded/fractured and the rest will be on the machined surface. In the present investigation, the interaction between the tool and reinforcement's i.e particles along the cutting path, particles above the cutting path and particles below the cutting path (Figure-2) with the advancement of cutting tool during machining at different cutting speed are discussed in detail.

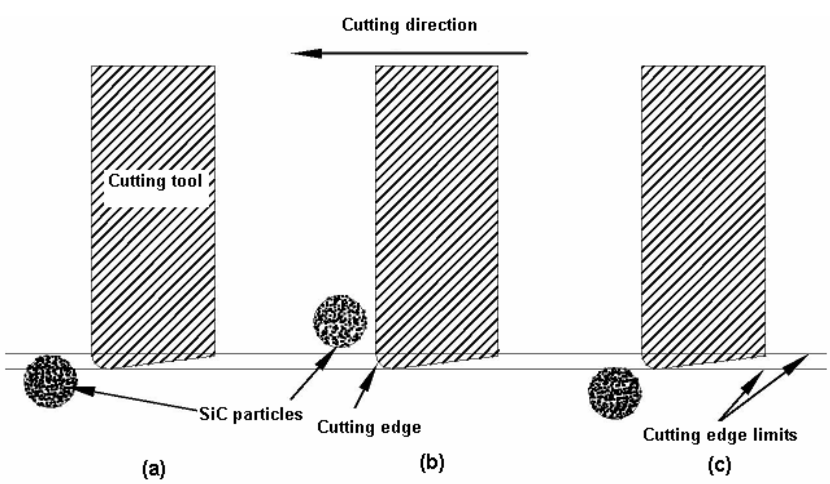

Figure-2. Particle locations with respect to the cutting path: particles (a) along, (b) above and (c) below the cutting path.

3.1 Evolution of stress field on SiC particles along, above and below the cutting path

3.1.1 SiC particles along the cutting path

The evolution of stress fields during machining of DRACs along the cutting path is demonstrated in Fig. 3. For a particle located in the lower part of the cutting edge, i.e., the center of particle is below the center of the cutting edge. Initially the compressive and tensile stresses are perpendicular and parallel, respectively, to the cutting edge in the matrix and particle in front of the cutting edge. This type of stress distribution may initiate fracture in the particle and debonding at the interface. With the advancement of the tool, the matrix between the upper part of the particle and tool becomes highly compressive while lower right interface of the particle becomes highly tensile. This indicates that an anticlockwise moment is acting on the particle, thus debonding of the particle may be expected with further advancement of the tool. Such stress distribution may initiate particle fracture if the stresses are high enough. With further advancement of the tool, the particle debonds and ploughs through the matrix making a cavity, then slides on the cutting edge, and becomes almost stress-free.

The stress field evolution for a particle located at the upper part of the cutting edge results in plastic flow of the matrix this particle has moved slightly upwards. Initially the matrix in between the particle and tool is under high compressive stress acting parallel to cutting direction with no tensile stress. On the other hand, a part of the particle and interface are under compressive stress along the cutting direction and under tensile stress perpendicular to the cutting direction. This type of stress distributions can lead to particle debonding or fracture. After interacting with the tool's rake face, the particle partially debonds and moves up with the chip. With further advancement of the tool it then interacts with a nearby particle and consequently both particles are under high compressive stress applying perpendicular to the rake face. This high compressive stress may cause fracture of the particle as well as wear on the tool rake face. Interaction of this particle with the second particle generates a similar stress distribution in the latter which can initiate its fracture and debonding. Additionally, stress in the surrounding matrix has reduced, possibly due to debonding of the particles.

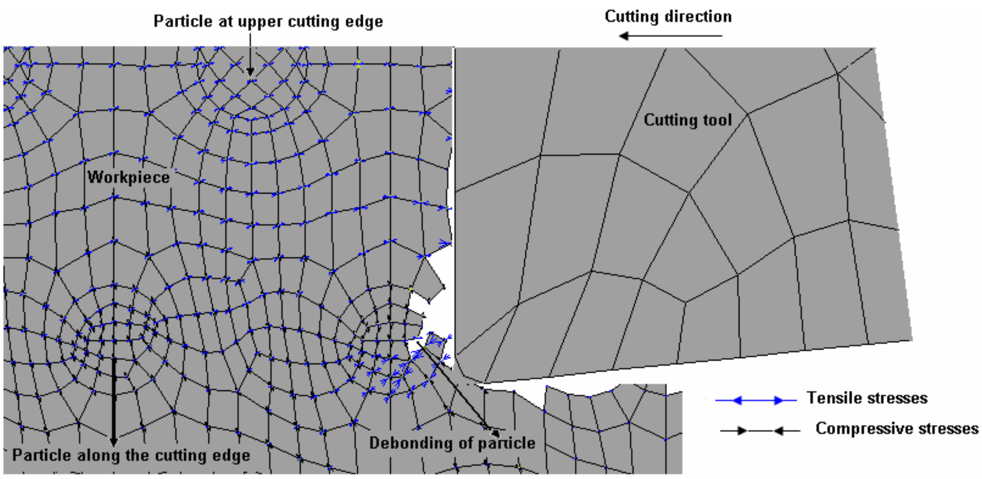

Figure-3. Evolution of stress fields for particles along the cutting path during machining of DRACs.

3.1.2 SiC particles above the cutting path

The evolution of stress field in the DRACs is presented in Figure-4. Initially high compressive stress field perpendicular to rake face through the particle and in the matrix in between particle and rake face is noted. At the same time, part of the particle and interface are under compressive stress (perpendicular to rake face) and tensile stress (parallel to rake face) as shown in Figure-4. As stated before, this type of stress distribution may initiate particle fracture and interface debonding. As the tool proceeds, it interacts and partially debonds the particle. The contact region with the rake face is under high compressive stress; hence fracture of the particle can be expected. At this stage the matrix in between this particle and next one is also under very high compressive stress. With further advancement of the tool, the first particle interacts with the next particle and moves up along the rake face under high compressive stress.

 ISSN 1819-6608
ARPN Journal of Engineering and Applied Sciences

www.arpnjournals.com

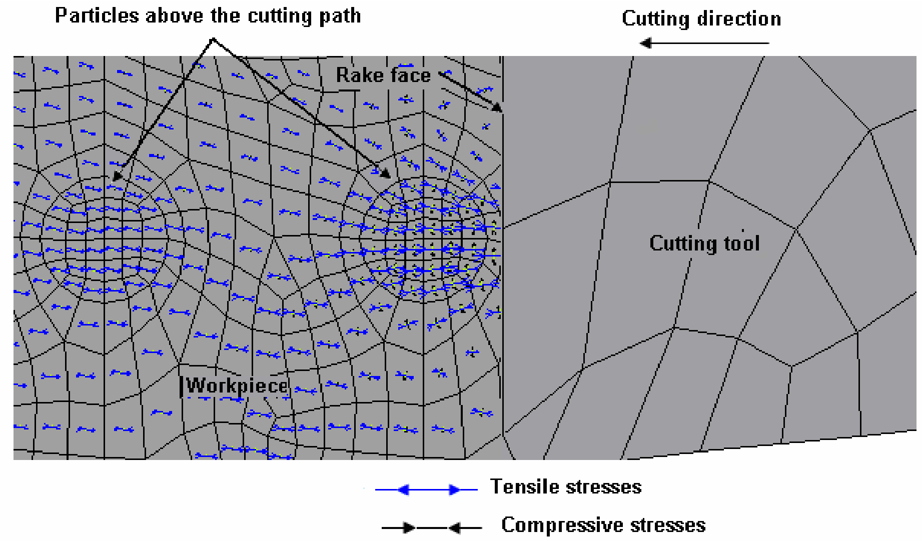

Figure-4. Evolution of stress fields for particles above the cutting path during machining of DRACs.

3.1.3 SiC particles below the cutting path

The stress distribution in the particle and matrix below the cutting edge has a direct influence on the residual stress of the machined surface. Figure-5 shows the evolution of stress field for a particle below the cutting edge. As the tool approaches the particle, the matrix in between the cutting edge and particle is under compressive stress acting in a radial direction to the cutting edge. However, the particle and particle-matrix interface are under compressive and tensile stresses which are acting in a radial direction to the cutting edge and parallel to the cutting edge. While the tool is passing over the particle, the direction of compressive stress remains radial to the cutting edge. On the other hand, the direction of tensile stresses in the particle becomes parallel to machined surface. It is also noted that the newly generated surface is under compressive residual stress which is parallel to the machined surface. Similar observations were also reported in an experimental study by [Yanming *et al.* (2003)], who machined SiC particulate reinforced MMC.

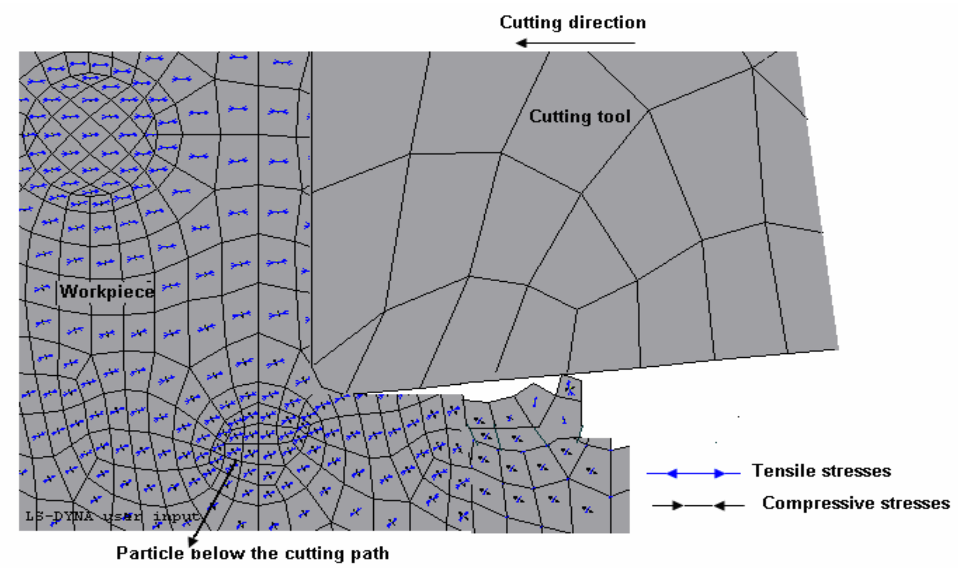

Figure-5. Evolution of the stress field for a particle below the cutting path during machining of DRACs.

3.2 Von-Mises stress distribution along the cutting path at different cutting speed

From the finite element simulations it is observed that particles in the lower part of the cutting edge initially interact with cutting edge and are then debonded leaving a cavity on the machined surface. They also take part in ploughing of the newly generated work surface. The particles in the upper part of the cutting edge slide over the rake face. It is expected that, with the increase of cutting speed, the impact between tool and particles generated high stress concentration. Similar observations were also reported in an experimental study by [El-Gallab *et al.* (1998)], who machined SiC particulate reinforced MMC.

Further Von-Mises stress distribution reveals that there was increase in stresses occurring during the machining of DRACs at 45m/min, 73m/min and 101m/min. An important feature observed in machining of DRACs is the occurrence of stress during the chip formation and tool interaction with the SiC particles. The influence of the cutting speed on the Von-Mises stress is analyzed keeping the depth of cut as constant for 0.5mm. Von Mises stress distribution for different speed is shown in the Figures (6a-6c). From these Figures it was observed that Von-misses stress during the turning operation of the DRACs is in the range of 2.815 to 988.5 MPa at the cutting speed of the 45m/min, as the speed increased to the 73m/min the range for the Von-Mises stress is 4.417Mpa to 1109.8 Mpa and for the speed of 101 m/min the range of stress is in between 6.657 to 1137.1 Mpa. The analysis revels that high levels of work hardening exists in the matrix around the hard SiC particles and thus a high stress is developed.

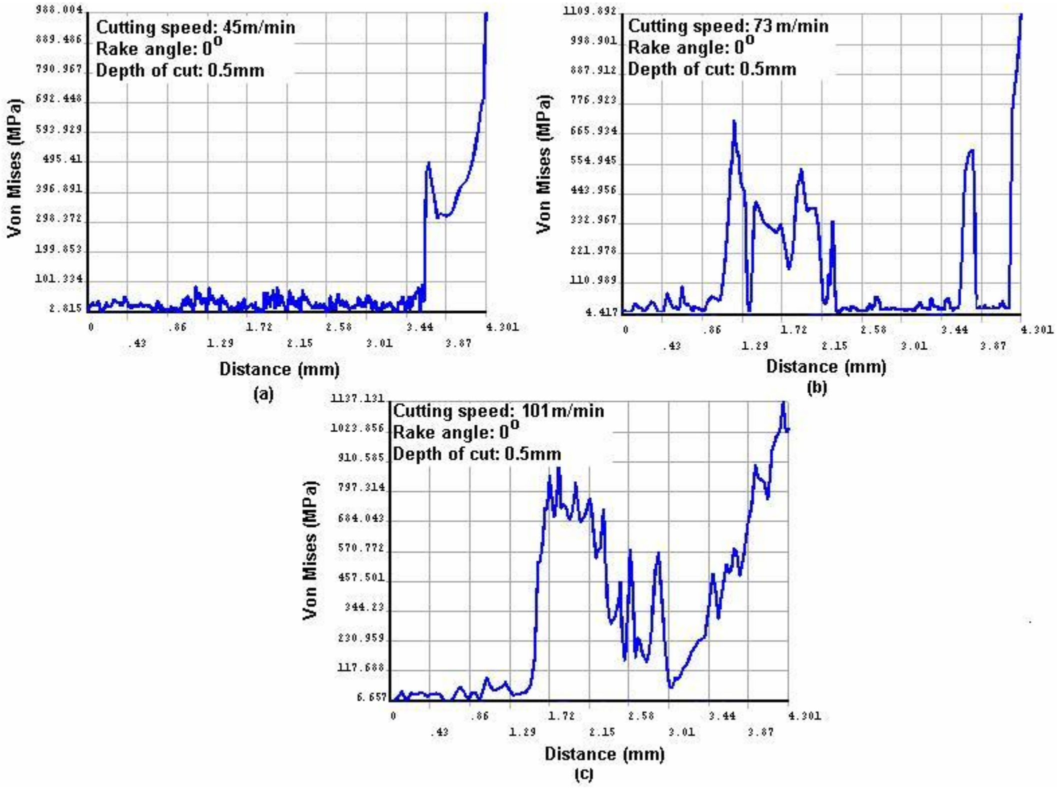

Figure-6. Von-Mises stress distribution on the matrix and SiC particle at different cutting speed and constant depth of cut.

5. CONCLUSIONS

This paper makes an interesting study in finite element modeling used for orthogonal cutting of DRACs. A complex issue, tool/particle interaction during machining was analyzed. The following conclusion can be drawn from this analysis:

- A finite element model was developed and used to simulate orthogonal machining of DRACs. It is believed that details afforded by this FE analysis will be great understanding of the particle's behavior during of machining of DRACs and can help in optimizing the process parameter.
- The simulation results of the Von Mises equivalent stress distribution on the DRACs depict a gradual increase in the stress concentration on particles as cutting speed increases and reaches a peak value as chip formation occurs.
- An increase in cutting speed from 45m/min to 73m/min seems to increase in the stresses by 121MPa and cutting speed from 45m/min to 101 m/min increased the stresses by 141MPa.
- The magnitude and distribution of stresses in the DRACs material and interaction of particles with the cutting tool are the main reasons for particle fracture and debonding during machining of DRACs.
- Newly generated surfaces are under compressive stress. Moreover, these surfaces are damaged due to cavities left by the pull-out of particles. These cavities are formed when particles located at the lower part of the cutting edge interact with the cutting tool.

6. REFERENCES

ANSYS/LS-DYNA Reference Manual, Release 10. Livermore Software Technology Corporation, Livermore, CA. www.lstc.com.

Beard T. 1998. Machining composites-new rules and tools. Modern Machine Shop. Vol. 619110, pp. 74-85.

Berrie P.G., Birkett F.N. 1980. The drilling and cutting of polymethyl methacrylate (Perpex) by CO_2 laser. Optics and Laser in Engineering, Applied Science Publisher Ltd., England. pp. 107-129.

Caprino G., Tagliaferri V. 1995. Damage devolvement in drilling glass fiber reinforced plastics. International Journal of Machine Tool and Manufacturing. 35(6): 817-829.

Evans A., Marchi C.S., Mortenson. 2003. A Journal of Metal Matrix Composites in Industry, an Introduction and a Survey, Kluwer, Boston.

El-Gallab M., Sklad M. 1998. Machining of Al/SiC particulate metal matrix composites, Part I: tool performance. Journal of Material Processing Technology Vol. 83, pp. 151-158.

Huda D., El Baradie M.A., Hashmi M.S.J. 1994. Analytical study for the stress analysis of metal matrix composites. Journal of Materials Processing Technology. Vol. 45, pp. 429-434.

Iwata K., Osakada K., Terasaka Y. 1984. Process modeling of orthogonal cutting by rigid-plastic finite element method. Journal of Engineering Materials and Technology, Transactions of ASME. Vol. 106, pp. 132-138.

Long S.G., Zhou Y.C. 2005. Thermal fatigue of particle reinforced metal-matrix composite induced by laser heating and mechanical load. Composites Science and Technology. Vol. 65, pp. 1391-1400.

Lin Z.C., Lin Y.Y., Liu C.R. 1991. Effect of thermal load and mechanical load on the residual stress of a machined surface. International Journal of Mechanical Sciences. Vol. 33, pp. 263-278.

Lin. Z.C., Lin. S.Y. 1992. A coupled finite element model of thermo-elastic-plastic large deformation for orthogonal cutting. Journal of Engineering Materials and Technology, Transactions ASME, Vol. 114, pp. 218-226.

Meijer G., Ellyin F., Xia Z. 2000. Aspects of residual thermal stress/strain in particle reinforced metal matrix composites. Composites: Part B. Vol. 31, pp.29-37.

Monaghan J., Brazil D. 1998. Modeling the flow processes of a particle reinforced metal matrix composite during machining. Composites. Vol. 29A, pp. 87-99.

Pramanik A., Zhang L.C., Arsecularatne J.A. 2006. Prediction of cutting forces in machining of metal matrix composites. International Journal of Machine Tools and Manufacturing. Vol. 46, pp.1795-1803.

Shetty Raviraj, Pai R.B., Rao S.S, Shenoy B.S. 2006. Application of finite element analysis in orthogonal cutting of aluminium metal matrix composites, In: Proceedings of International conference on Advances in Mechanical Engineering, ICAME, Chennai, India.

Yanming Q., Bangyan Y. 2003. The effect of machining on the surface properties of SiC/Al composites. Journal of Materials Processing Technology. Vol. 138(1-3): 464-467.

Zhu Y., Kishawy H.A. 2005. Influence of alumina particles on the mechanics of machining metal matrix composites. International Journal of Machine Tools and Manufacturing. Vol. 45, pp. 389-398.

Zhang Z.F, Zhang L.C., Mai Y.W. 1995. Particle effects on friction and wear of aluminium matrix composites. Journal of Materials Science. 30(23): 5999-6004.